Numerical Analysis of the 4 K Regenerator in a Pulse Tube Cryocooler

Y.Zhao[1,2], W.Dai[1], Y.Chen[1], X.Wang[1], E.Luo[1]

[1]Key Laboratory of Cryogenics, Technical Institute of Physics and Chemistry, Chinese Academy of Sciences, Beijing, 100190 China
[2]University of Chinese Academy of Sciences, Beijing 100049, China

ABSTRACT

The numerical simulation of a 4 K pulse tube cryocooler is difficult due to its complexity of nature. The main difficulty comes from the oscillatory flow combined with the real gas effects. In this paper, the numerical simulation of the 4 K regenerator in a pulse tube cryocooler with a relatively high frequency has been performed with the commercial CFD software, FLUENT [1]. FLUENT takes into account the non-ideal gas properties of ^{4}He, the properties of the magnetic regenerative material, and the heat transfer inside the heat exchanger and regenerator. Interesting features such as the acoustic work flow, temperature distribution, the volume flow, etc., have been systematically studied. A cooling power of 0.36 W was obtained numerically at the temperature of 4.2 K. The study takes a deeper look into the working mechanism of a 4 K pulse tube cryocooler as well as setting the basis for optimizing a pulse tube cooler driven by a Vuillemier type thermal compressor.

INTRODUCTION

Cryocoolers working at liquid helium temperatures could be used in the application fields of space exploration, military, medical and low-temperature physics. Especially, for many applications, a 4 K pulse tube cryocooler is a potential candidate because of the merits of no cryogenic moving components. Owing to the advances in cooler design and the development of magnetic regenerative materials [2-4], a cooling temperature below 4 K was first obtained with a three-stage Gifford McMahon (G-M) type pulse tube refrigerator [5]. In 2004, a new low temperature of 2.13 K near the lambda line of ^{4}He was obtained [6]. Using ^{3}He as a working fluid in the 2nd stage, a minimum temperature of 1.27 K was later achieved. With an electrical input power of 1.3 kW and 4.3 kW to the 1st and 2nd stage respectively, the 2nd stage provides a cooling power of 42 mW at 2.0 K and 518 mW at 4.2 K [7]. These results show the promising application potential of pulse tube coolers for cooling below 4.2 K.

Nowadays, G-M cryocoolers or G-M type pulse tube cryocoolers are the leading technology to generate temperatures in the 4 K region for small scale applications [8,9]. The use of oil-lubricated compressors and switch valves leads to low thermal efficiency, low power density and the need for regularly scheduled maintenance. To overcome these shortcomings, the Stirling type cryocooler has been one of the focuses of research [10-12]. The American company, Lockheed Martin Inc., and Zhejiang University of China have developed a Stirling type cryocooler which

Cryocoolers 18, edited by S.D. Miller and R.G. Ross, Jr.

can reach the liquid helium temperatures [13,14], but the refrigeration capacity is very small and the thermal efficiency is much lower than that of G-M cryocoolers. One of the fundamental reasons is that in the liquid helium temperature region the working frequency of Stirling type cryocoolers is quite high, which leads to the increased losses especially inside the low temperature regenerator packed with spheres. Dai, et al.[15] thus proposed a modified version of pulse tube cryocooler driven by a Vuillemier (VM) type thermal compressor. By using the temperature difference between the environment and a cryogenic temperature, a pressure wave could be generated to drive a pulse tube cold head.

This paper mainly studies the lowest regenerator section of a 4 K pulse tube cryocooler numerically in order to better understand the processes occurring in the low temperature regenerator and analyze the loss mechanism of the acoustic work and the cooling power. Specifically, the working frequency, 5 Hz, is apparently higher than that of a conventional GM type cryocooler for the purpose of increasing the specific power. The next section will introduce the physical and mathematic models, and following section will give the results and discussions. Finally, some conclusions are drawn.

PHYSICAL AND MATHEMATIC MODELS

As addressed earlier, the regenerator section (between 20 K and 4.2 K) to be studied is part of a VM type pulse tube cryocooler system to be introduced in another paper from our group. In the system, the dynamic pressure is supplied by the VM thermal compressor. The regenerator studied is the lowest section of the regenerator, which is taken out and sandwiched between two heat exchangers to investigate how well it will perform with a given input acoustic work or pressure ratio. The whole system is expected to provide a cooling power of 0.2 W at 4.2 K.

According to Figure 1, the model includes five main regions: compression space, hot heat exchanger (HHX), regenerator, cold heat exchanger (CHX) and the expansion space. The regenerator is filled with the magnetic regenerative material $HoCu_2$, which has a sphere diameter of 0.3 mm. The diameter of the regenerator is 18 mm, and the length of the hot heat exchanger (HHX), regenerator and cold heat exchanger (CHX) are 15 mm, 80 mm and 8 mm, respectively. The main structure parameters are listed in the following Table 1.

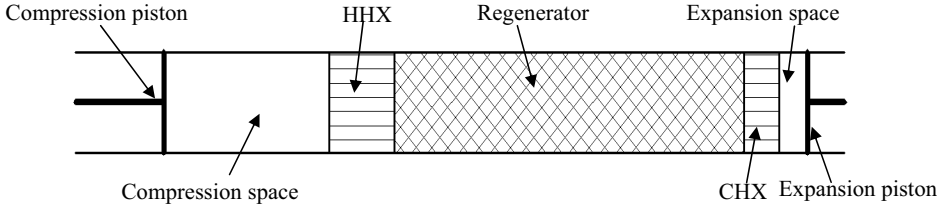

Figure 1. Schematic physical model of cold head of a 4 K pulse tube cryocooler

Table 1. Main structure parameters

Component	Dimensions
Compression space	Volume 11.95×10^{-6} m^3
Hot heat exchanger	Diameter 18 mm, Length 15 mm, Porosity 0.56
Regenerator	Diameter 18 mm, Length 80 mm, Filler $HoCu_2$, Sphere diameter 0.3 mm, Porosity 0.39
Cold heat exchanger	Diameter 18 mm, Length 8 mm, Porosity 0.33
Expansion space	Volume 2.54×10^{-6} m^3

The following assumptions are used in the simulation: (1) the gas flow is laminar and axisymmetric; (2) the wall temperature of cold and hot heat exchanger is constant; (3) the thermal conduction losses through the walls are ignored. The governing equations, including the continuity equation, momentum equation and energy equation, are given as follows.

Continuity equation:

$$\frac{d\rho_g}{dt} + \nabla \cdot (\rho_g \vec{u}) = 0 \tag{1}$$

Momentum equations:

$$\frac{\partial}{\partial t}(\rho_g \vec{u}) + \nabla \cdot (\vec{u}\vec{u}) = -\nabla P + -\rho_g g + s \tag{2}$$

Energy equation for the gas zone:

$$\frac{\partial}{\partial t}\left(\varphi \rho_g E_g\right) + \nabla \cdot (\vec{u}(\varphi \rho_g E_g + p)) = \nabla \cdot (\varphi k_g \nabla T_g + (\vec{\tau} \cdot \vec{u})) + h_{gs} A_r (T_s - T_g) \tag{3}$$

Energy equation for the solid zone:

$$\frac{\partial}{\partial t}\left((1-\varphi)\rho_s E_s\right) = \nabla \cdot ((1-\varphi) k_s \nabla T_s) + h_{gs} A_r (T_s - T_g) \tag{4}$$

Equation of state for ^{4}He

$$H = f(T, P) \text{ or } T = f(h, P) \tag{5}$$

where ρ_g is the density of ^{4}He, k_g is the thermal conductivity of ^{4}He, $\vec{\tau}$ is the viscosity force vector, φ is the porosity; $\vec{u}$ is the velocity vector, S is a resistance source term of the momentum equations for porous region. E_g is the total gas energy; A_r is the interfacial area density; T_g is the temperature of the gas, ρ_s is the density of $HoCu_2$, k_s is the thermal conductivity of $HoCu_2$, T_s is the temperature of the solid, and P is the pressure.

Real gas properties impose strong effects on regenerators. The pressure-independent enthalpy flow generally induces serious losses and consequently decreases the refrigeration efficiency at temperature around 4 K. Meanwhile, the density, thermal conductivity, viscosity and specific heat of ^{4}He change dramatically with temperature, which would easily cause the calculation to diverge. The real gas properties of ^{4}He are obtained from the NIST12 helium database [16]. The corresponding source code of helium thermal physical properties has been incorporated within the CFD simulation software, Fluent.

The specific heat for the regenerative material $HoCu_2$ used in the present simulation is shown in Figure 2. The data of the materials is taken from the website http://www.cryogenics.nist.gov. It can be seen from Figure 2 that the specific heat has two peak values at temperature around 9 K and 12 K. Figure 2 also shows the ratio of the heat capacity of the unit volume between $HoCu_2$ and ^{4}He, which increases almost monotonically with temperature above 10 K.

For the model, the left boundary is the surface of the compression piston. The motion of the piston is given by

$$v(t) = v_1 \cos(2\pi f t) \tag{6}$$

The right boundary is the surface of the expansion piston. The motion of the piston is given by

$$v(t) = v_2 \cos(2\pi f t - \theta) \tag{7}$$

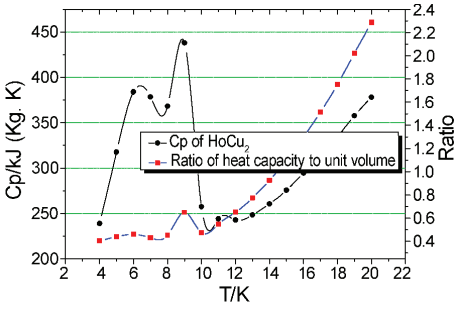

Figure 2. Dependence of Cp on temperature for $HoCu_2$

where v_1 is the velocity amplitude of compression piston and v_2 is the velocity amplitude of expansion piston, f is the frequency, and θ is the phase difference between the pistons.

In this paper, the compression piston velocity amplitude v_1 is 0.33 m/s, which means a swept volume of 5.4 cm^3. The expansion piston velocity amplitude v_2 is 0.16 m/s. The frequency is 5 Hz, which can bring a relative higher energy density The phase difference θ between the compression and expansion piston is 0.77 radians, e.g., -44°.

The heat exchangers and the regenerator are all treated as porous media. To consider the non-ideal properties of materials of low temperature in the regenerator, a non-thermal equilibrium model is used to simulate the heat transfer between the gas and the solid. Empirical correlations for the heat transfer and friction factor are given as follows.

Nusselt Number [17]:

$$\mathrm{Nu} = 1 + 0.48\mathrm{Pe}^{0.65} \tag{8}$$

Friction factor:

$$\alpha = \frac{d_p^2}{150}\frac{\varphi^3}{(1-\varphi)^2} \tag{10}$$

$$C_2 = \frac{3.5}{d_p}\frac{(1-\varphi)}{\varphi^3} \tag{11}$$

where $\mathrm{Pe} = RePr$; d_p is the sphere diameter of $HoCu_2$; φ is the porosity; $1/\alpha$ is the coefficient of viscous resistance; C_2 is the coefficient of inertial resistance. The wall temperature of the HHX is set to 20 K, and the CHX wall is set to 4.2 K. All the other walls are treated as adiabatic.

RESULTS AND DISCUSSION

The commercial CFD code FLUENT is used to run all of the simulations. A 2D axisymmetric model has been established to simulate the model shown in Fig.1. The total number of mesh cells is 8,450. Pressure based solver is used to solve the compressible oscillating flow. The heat exchangers and the regenerator are all treated as porous media. To consider the non-ideal properties of materials under low temperature in the regenerator, non-thermal equilibrium model is used to simulate the heat transfer between the gas and the solid. Piston movements which are governed by Eq. (6) and (7) are simulated by dynamic mesh technology. A first order implicit scheme is used for the dynamic mesh calculation. A small time step is required to avoid large artificial losses. The Pressure-Implicit with Splitting of Operators (PISO) pressure-velocity coupling scheme has been used for updating pressure and correcting the velocity components. For spatial discretization, the PRESTO! Algorithm is used for pressure and the 2rd order upwind scheme for others. Grid independence has been performed before final results are given.

Labview™ is used to analyze the average value, the first-order amplitude and the phase after the simulation is run. With the defined boundary condition, the working pressure ratio is about 1.37. The temperature distribution, the acoustic work flow, the volume flow rate and the axial thermal conduction losses have been statistically analyzed. The temperature distribution has been compared with the numerical results of Sage software.

Figure 3 shows the dynamic pressure drop along the regenerator. In the compression space the pressure amplitude is 1.96×10^5 Pa. The pressure amplitude drop in the hot heat exchanger, regenerator and cold heat exchanger is 1592 Pa, 11257 Pa and 775 Pa respectively. Inside the expansion space, the dynamic pressure amplitude is 1.8×10^5 Pa. Figure 4 gives the acoustic work distribution across the regenerator. At the left side the acoustic work is 8.14 W and at the right side the acoustic work is 3.26 W.

Figure 5 shows the volume flow rate across the regenerator. The compression piston provides a volume flow rate of 8.79×10^{-5} m^3/s. At the left side of the regenerator, the amplitude of the volume flow rate is 7.78×10^{-5} m^3/s, while at the right side of the regenerator; the amplitude of the volume flow rate is 3.80×10^{-5} m^3/s. Figure 6 shows the phases of pressure wave and the volume flow rate, and the difference between them.

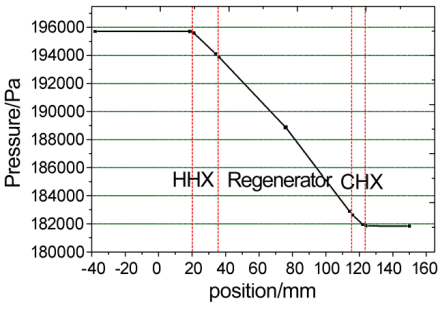

Figure 3. The pressure amplitude drop

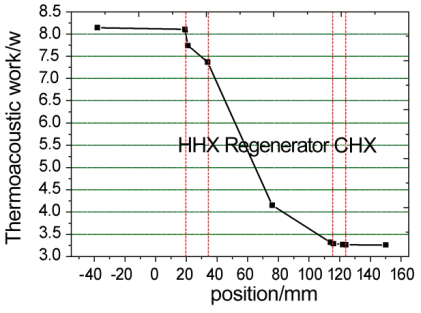

Figure 4. The acoustic work distribution

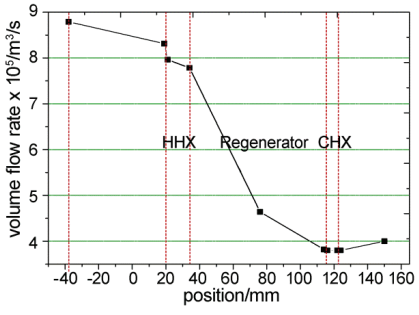

Figure 5. Volume flow rate along the regenerator

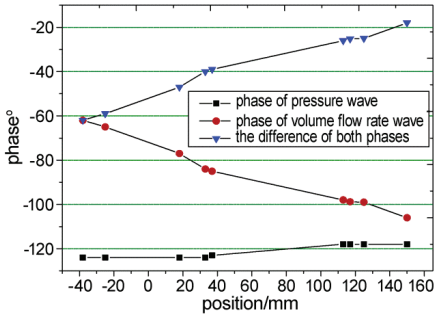

Figure 6. Phase distribution along the regenerator

Figure 7 shows the temperature distribution of ^{4}He fluid inside the regenerator. It can be seen that in the left half (near the hot heat exchanger) of the regenerator, the gradient is big, while in the right half (near the cold heat exchanger) the gradient is relatively small. The phenomenon is well known in G-M type cryocoolers.

At the same time, the axial thermal conduction losses have been analyzed. Considering the porosity and sphere-packed configuration of regenerator, the axial thermal conductivity of the bulk material has been corrected. Figure 8 shows the values of the axial heat conduction losses at different positions of the regenerator, which is related to the temperature gradient. At the left-most, middle and right-most positions, the value is 0.19 W, 0.10 W and 0.03 W respectively.

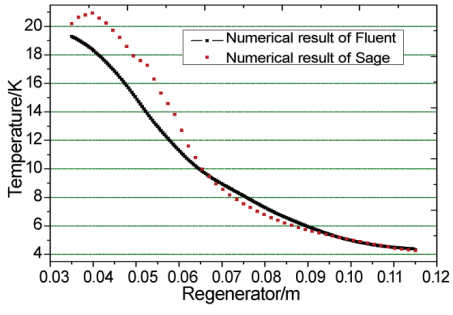

Figure 7. The average temperature distribution in the regenerator

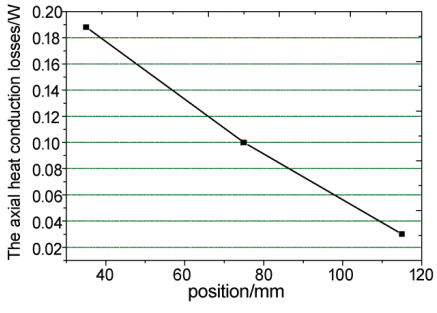

Figure 8. The axial thermal conduction loss along the regenerator

Table 2. The statistic numerical result

The average pressure	The pressure ratio	The input acoustic work	The cooling power	The relative Carnot efficiency
1.2 MPa	1.37	8.14 W	0.36 W	27.8%

A generalization of the statistic numerical results is shown in the Table 2. At an average pressure of 1.2 MPa and the pressure ratio of 1.37, the cooling power at 4.2 K is 0.36 W, which corresponds to a relative Carnot efficiency of 27.8%.

CONCLUSION

A numerical simulation has been performed on the 4 K regenerator of a pulse tube cryocooler, which takes into account the non-ideal gas properties of ^{4}He, the temperature dependence of specific heat of regenerative materials, and heat transfer inside the heat exchanger and regenerator. The preliminary simulation revealed the features associated with the regenerator working at such a low temperature. A cooling power of 0.36 W at 4.2 K was numerically obtained and the relative Carnot efficiency is 27.8%. Currently, a more systematic study is underway for more in-depth analyses. Meanwhile, experiments are being prepared for validating the simulations.

ACKNOWLEDGMENT

This work is financially supported National Natural Science Foundation with project number 51376187 and the Institute Supervisor Fund of Technical Institute of Physics and Chemistry of Chinese Academy of Sciences. Support of K.C.Wong Education Foundation of Hong Kong are greatly acknowledged.

REFERENCE

1. ANSYS, INC. "ANSYS FLUENT User's Guide," Published in the USA (2011).
2. Mikulin, E.L, Tarasov, A.A. and Shkrebyonoch, M.P. "Low temperature expansion pulse tubes," *Adv. in Cryogenic Engineering,* Vol. 29, Plenum Publishing Corp., New York (1984), p. 629.
3. Zhu, S.W., Wu, P.Y. and Chen, Z.Q. "Double inlet pulse tube refrigerator: an important improvement," *Cryogenics,* Vol. 30 (1990), p. 514.
4. Hashimoto, T., Ogawa, M., and Hayashi, A. "Recent progress on rare earth magnetic regenerator material," *Adv. in Cryogenic Engineering,* Vol. 37B, Plenum Publishing Corp., New York (1992), p. 859.
5. Matsubara, Y. and Gao, J.L. "Novel configuration of three-stage pulse tube refrigerator for temperatures below 4 K," *Cryogenics,* Vol. 34 (1994), p. 259.
6. Thummes, G., Bender, S. and Heiden, C., "Approaching the ^{4}He lambda line with a liquid nitrogen prccooled two-stage pulse tube refrigerator," *Cryogenics,* Vol. 36 (1996), p. 709.
7. Jiang a, N., Lindemann, U., Giebeler, F., Thummes, G., "A ^{3}He pulse tube cooler operating down to 1.3 K," *Cryogenics,* Vol. 44 (2004), pp. 809–816.
8. Radebaugh R, Huang YH, O'Gallagher A, et al. "Calculated regenerator performance at 4 K with helium-4 and helium-3," *Cryogenics,* Vol. 53 (2008), pp. 225–234.
9. Zhi, X.Q., Han, L., etc. "A three-stage Stirling pulse tube cryocooler reached 4.26 K with He-4 working fluid," *Cryogenics,* Vol. 58 (2013), pp. 93–96.
10. Sun, D.M., Dietrich, M., Thummes, G., "High-power Stirling-type pulse tube cooler working below 30 K," *Cryogenics,* Vol. 49 (2009), pp. 457–462.

11. Wang, C., "Numerical analysis of 4 K pulse tube coolers: Part I. Performances and internal processes," *Cryogenics,* Vol. 37 (1997) 207-213.

12. Wang, C., "Numerical analysis of 4 K pulse tube coolers: Part II. Performances and internal processes," *Cryogenics,* Vol. 37 (1997), pp. 215-220.

13. Qiu LM, Cao Q, etc. "A three-stage Stirling pulse tube cryocooler operating below the critical point of helium-4," *Cryogenics*, Vol. 51 (2011), pp. 609 – 12.

14. Qiu LM, Cao Q, Zhi XQ, et al. "Operating characteristics of a three-stage Stirling pulse tube cryocooler operating near 5 K*," Cryogenics,* Vol. 52 (2012), pp.382 – 8.

15. Dai, W., Wang, X., Zhao, Y., Luo, E., Zhou, Y., "Characteristics of a VM Type Thermal Compressor for Driving a Pulse Tube Cooler," *Cryocoolers 18*, ICC Press, Boulder, CO (2015), (this proceedings).

16. Lemmon, E.W., Peskin, A.P., McLinden, M.O., Friend D.G., *NIST Standard Reference Database 12: Thermodynamic and Transport Properties of Pure Fluids, Version 5.0,* National Institute of Standards, Boulder, CO., (2000)

17. Gedeon. D., *Sage User's Guide-Stirling, Pulse-Tube and Low-T Cooler Model Classes*, Gedeon Associates, Athens, OH (2011).